Journal of Clinical and Translational Pathology **2026**
DOI: 10.14218/JCTP.2025.00043

Research Letter

An Infantile Low-grade Mesenchymal Tumor with Fibrohistiocytic Differentiation and Co-occurring *CSF1R* Mutation and *MALAT1* Rearrangement

Min Li, Yu Dong and Anjia Han*

Department of Pathology, the First Affiliated Hospital, Sun Yat-Sen University, Guangzhou, Guangdong, China

Received: October 12, 2025 | **Revised:** December 14, 2025 | **Accepted:** March 03, 2026 | **Published online:** March 20, 2026

Citation of this article: Li M, Dong Y, Han A. An Infantile Low-grade Mesenchymal Tumor with Fibrohistiocytic Differentiation and Co-occurring *CSF1R* Mutation and *MALAT1* Rearrangement. J Clin Transl Pathol 2026. doi: 10.14218/JCTP.2025.00043.

Fibrohistiocytic tumors in children and adolescents represent a heterogeneous group of mesenchymal neoplasms. Their biological behavior spans a broad spectrum, ranging from benign lesions to malignant sarcomas, and they are unified by a common histologic differentiation spectrum encompassing fibroblastic, myofibroblastic, and histiocytic-dendritic lineages.[1] The molecular pathological landscape of these tumors is rapidly expanding with the application of next-generation sequencing (NGS) technologies. This report details a case of an infantile low-grade mesenchymal tumor with fibrohistiocytic differentiation harboring a unique co-occurring *CSF1R* mutation and *MALAT1* rearrangement, which has not been previously reported. This report expands the molecular landscape of infantile fibrohistiocytic tumors and provides insights into potential pathogenic mechanisms.

The patient was a nine-month-old male infant. Two months ago, a physical examination revealed a mass in the right axilla. Subsequently, the infant underwent excision of the right axillary mass at a local children's hospital. The pathological sections of the mass were submitted to our Department of Pathology for consultation. Two months after the axillary mass resection, an ultrasound examination at our institution revealed a hypoechoic nodule in the right paravertebral region (Supplementary Fig. 1), which was considered indicative of postoperative tumor recurrence based on the patient's history. The patient subsequently underwent percutaneous biopsy under ultrasound guidance in the Department of Ultrasound at our hospital. However, the pathological morphology (Supplementary Fig. 2) and immunohistochemical findings (Supplementary Fig. 3) of the biopsy specimen were inconsistent with those of the original right axillary mass, suggesting a different tumor. The patient was discharged following the implantation of a venous port-access device at our institution, and chemotherapy was not initiated. The patient was subsequently seen at Guangzhou Children's Hospital, where a paravertebral mass resection was performed. The Department of Pathology at the children's hospital diagnosed the lesion as neuroblastoma. Immunohistochemical results showed that tumor cells were positive for Phox2B and ATRX, negative for C-myc and ALK, with a Ki-67 index of 5%. Fluorescence *in situ* hybridization (FISH) analysis demonstrated no amplification of the *MYCN* gene. Recent chest DR imaging of the child revealed no abnormalities in the heart, lungs, or diaphragm, and the distal tip of the infusion port was positioned at the level of the sixth thoracic vertebra (Supplementary Fig. 4). One year after the resection of the axillary mass, there has been no recurrence or metastasis of the right axillary lesion, and the child remains alive. This report primarily focuses on the right axillary mass.

The resected axillary mass measured 1.8 cm × 1.7 cm × 1 cm and presented a grayish-white, nodular cut surface. Histopathological examination of the axillary mass revealed that the tumor tissue was located within the dermis, with relatively well-defined borders and focal extension into the subcutaneous adipose tissue (Fig. 1a). The tumor cells exhibited a slightly storiform growth pattern (Fig. 1b and c). The tumor cells were predominantly short and spindle-shaped, with lightly eosinophilic cytoplasm and irregular nuclear contours. Small nucleoli were discernible in a subset of cells, and the chromatin exhibited a variably coarse-to-fine texture. Mitotic figures were frequent, approximately 20 per 2 mm^2, and pathological mitotic figures were also identified (Fig. 1d–g). Focal hemosiderin deposition was noted (Fig. 1h).

Immunohistochemical staining revealed that the tumor cells exhibited strong positivity for CD163 (Fig. 2a), approximately 40% positivity for Cyclin D1 (Fig. 2b), and partial positivity for CD10. Notably, BRG1 expression was retained without loss. The tumor cells also exhibited positivity for CD99, CD4, CD31, and CD68. Conversely, negative results were obtained for CK, SMA, desmin, calponin, CD34, BCOR, MUC4, ALK, TLE1, CR, SOX10, CD30, granzyme B, TIA-1, CD3, CD45, CD1a, P53, TRK, Bcl-2, S-100, EMA, ERG (Fig. 2c), WT1 (Fig. 2d), MPO (Fig. 2e), as well as NKX2.2 (Fig. 2f), CD79a, and CD117 (Fig. 2g), with a Ki-67 proliferation index of approximately 40% in hotspot regions (Fig. 2h). FISH analyses showed negative results for *CIC* gene breakage (19q13) (Fig. 3a), *EWSR1* gene rearrangement (Fig. 3b), and *ETV6::NTRK3* fusion genes (t(12;15)) (Fig. 3c). NGS of DNA and RNA from the tumor tissue identified a *CSF1R P566_N572del* mutation and a *MALAT1*/intergenic rear-

*Correspondence to: Anjia Han, Department of Pathology, the First Affiliated Hospital, Sun Yat-sen University, 58 Zhongshan Road II, Guangzhou, Guangdong 510080, China. ORCID: https://orcid.org/0000-0003-3357-5348. Tel: +86-13423609339, E-mail: hananjia@mail.sysu.edu.cn

Copyright: © 2026 The Author(s). This article has been published under the terms of Creative Commons Attribution-Noncommercial 4.0 International License (CC BY-NC 4.0), which permits noncommercial unrestricted use, distribution, and reproduction in any medium, provided that the following statement is provided. "This article has been published in *Journal of Clinical and Translational Pathology* at https://doi.org/10.14218/JCTP.2025.00043 and can also be viewed on the Journal's website at https://www.xiahepublishing.com/journal/jctp".

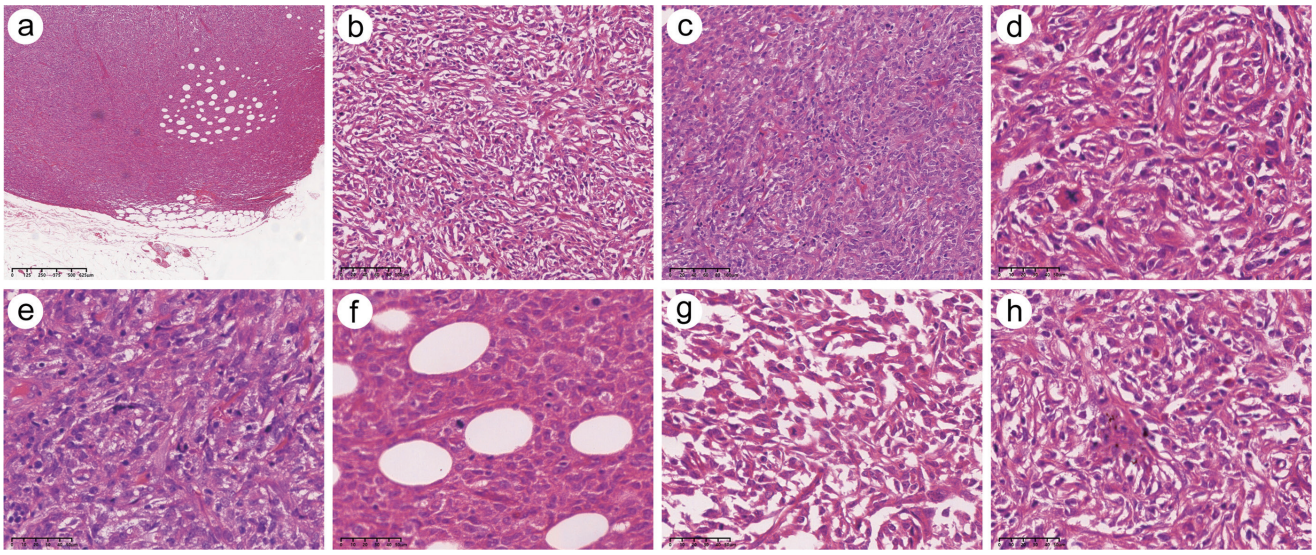

Fig. 1. Representative hematoxylin and eosin (H&E) stains of the axillary mass tissue: the tumor tissue was located within the dermis, with relatively well-defined borders and focal extension into the subcutaneous adipose tissue (a, original magnification, ×40; scale bar, 125 μm). The tumor cells exhibited a slightly storiform growth pattern (b–c, original magnification, ×200; scale bar, 20 μm). The tumor cells were predominantly short and spindle-shaped with irregular nuclear contours, exhibited frequent mitotic figures (approximately 20 per 2 mm^2), and displayed lightly eosinophilic cytoplasm (d–g, original magnification, ×400; scale bar, 10 μm). Focal hemosiderin deposition was noted (h, original magnification, ×400; scale bar, 10 μm).

rangement, with the intergenic region located on chromosome 19q13. The *MALAT1* break-apart probe (*MALAT1* red break-apart probe and *MALAT1* green break-apart probe) was used to assess 100 cells. The results showed 6% with a 1R1G signal pattern, 35% with a 1R1G1F pattern, and 3% with a 1R1G2F pattern, indicating the detection of a *MALAT1* gene rearrangement (Fig. 3d). Based on a comprehensive evaluation of the histological characteristics, immunohistochemical profile, FISH results, and NGS data, a final diagnosis of an infantile low-grade mesenchymal tumor with fibrohistiocytic differentiation and co-occurring *CSF1R* mutation and *MALAT1* rearrangement was established.

For this case, the differential diagnosis should encompass infantile fibrosarcoma, spindle cell synovial sarcoma, inflammatory myofibroblastic tumor, *CIC*-rearranged sarcoma, *BCOR*-altered sarcoma, undifferentiated round cell sarcoma with Ewing-like morphology, malignant peripheral nerve sheath tumor, spindle cell rhabdomyosarcoma, and leiomyosarcoma. Despite the patient's age and tumor morphology suggestive of infantile fibrosarcoma, the diagnosis was not supported by negative TRK and the absence of *ETV6::NTRK3* fusion on FISH.[2] Synovial sarcoma was ruled out based on negative expression of epithelial markers (CK, EMA) and TLE1. ALK negativity by immunohistochemistry

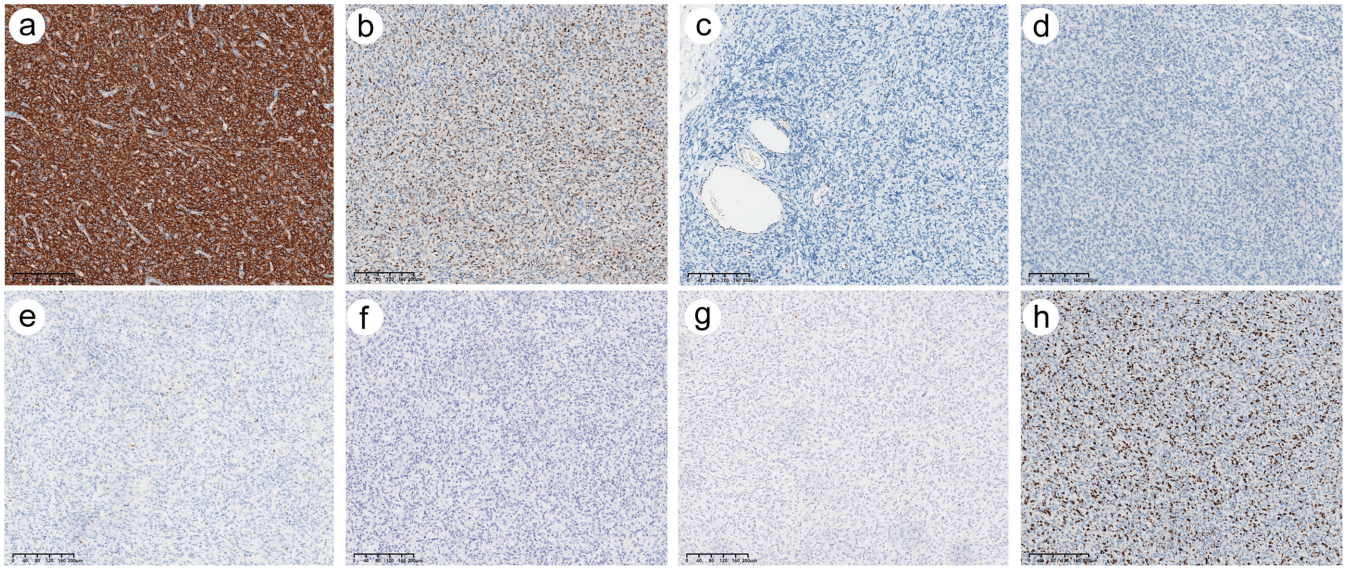

Fig. 2. Representative immunohistochemical stains of the axillary mass tissue (original magnification, ×100; scale bar, 40 μm). The tumor cells exhibited strong positivity for CD163 (a), approximately 40% positivity for Cyclin D1 (b), and a Ki-67 proliferation index of approximately 40% in hotspot regions (h). Staining results were negative for ERG (c), WT1 (d), MPO (e), NKX2.2 (f), and CD117 (g).

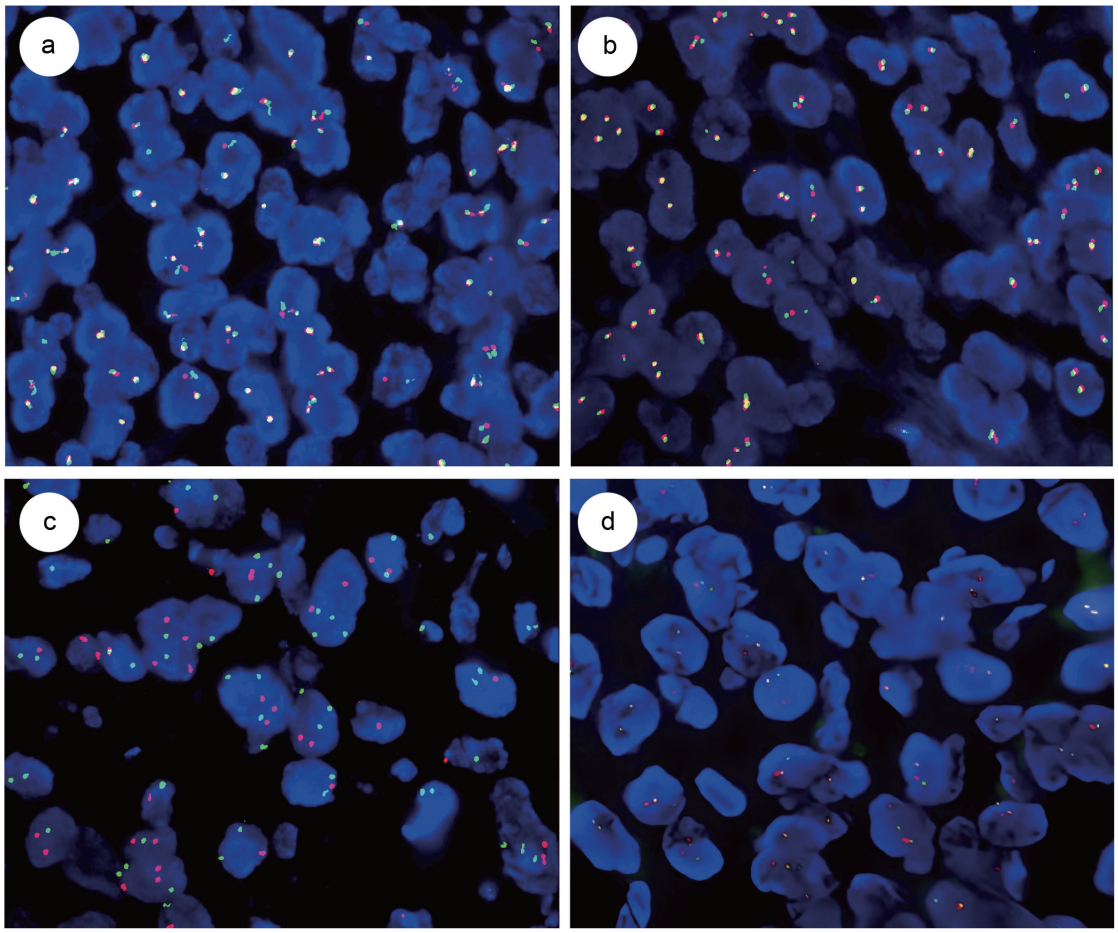

Fig. 3. Fluorescence *in situ* hybridization (FISH) analyses showed negative results for *CIC* gene breakage (19q13) (a), *EWSR1* gene rearrangement (b), and *ETV6::NTRK3* fusion genes (t(12;15)) (c). The *MALAT1* break-apart probe (*MALAT1* red break-apart probe and *MALAT1* green break-apart probe) was used to assess 100 cells. The results showed 6% with a 1R1G signal pattern, 35% with a 1R1G1F pattern, and 3% with a 1R1G2F pattern, indicating the detection of a *MALAT1* gene rearrangement (d).

and lack of inflammatory infiltrate argued against inflammatory myofibroblastic tumor.[3] *CIC*-rearranged sarcoma and *BCOR*-altered sarcoma were excluded due to FISH analysis demonstrating no *CIC* rearrangement and nonreactive BCOR immunohistochemistry, respectively.[4] The spindle cell morphology, absence of NKX2.2 expression, and negative *EWSR1* FISH contradicted undifferentiated round cell sarcoma with Ewing-like morphology.[5] Negative expression of neural markers (S-100 protein, SOX10) excluded malignant peripheral nerve sheath tumor. Additionally, spindle cell rhabdomyosarcoma and leiomyosarcoma were excluded because desmin, SMA, and calponin by immunohistochemistry were negative, and there was a lack of evidence of myogenic differentiation. The CD68/CD163-positive immunophenotype prompted consideration of fibrohistiocytic tumors, such as tenosynovial giant cell tumor (TGCT). However, this possibility was excluded based on atypical clinical presentation (occurring in the axillary soft tissue of an infant), inconsistent histological features (lacking the characteristic admixture of osteoclast-like giant cells and foamy histiocytes), and a distinct molecular profile (co-occurring *CSF1R* mutation and *MALAT1* rearrangement, which is fundamentally different from the *CSF1* fusions characteristic of TGCT.[6,7] Other *MALAT1*-rearranged tumors, such as gastric plexiform fibromyxoma, were also considered but dismissed due to the distinct anatomic site, bland histology with a plexiform growth pattern, and specific *MALAT1::GLI1* fusion.[8] In conclusion, this tumor cannot be classified into any known existing category. The *CSF1R* mutation co-occurring with *MALAT1* rearrangement in this case may define a novel molecular subtype.

The *CSF1R* gene encodes a tyrosine kinase receptor regulating macrophage proliferation and differentiation.[9] Mutational activation of the *CSF1/CSF1R* axis recruits tumor-associated macrophages (evidenced by CD68/CD163 positivity) and promotes tumor progression via immunosuppression and angiogenesis.[10] In this case, the *CSF1R* mutation is likely responsible for the tumor cells exhibiting a macrophage-like immunophenotype. Notably, CSF1R inhibitors (e.g., pexidartinib, ABSK021) demonstrate therapeutic efficacy in TGCTs,[11] suggesting potential targeted therapy applicability in this molecular context. In contrast, *MALAT1*, a long non-coding RNA, regulates cancer-related processes, including proliferation, metastasis, and drug resistance, by interacting with transcription factors, growth factors, and epigenetic modifiers.[12] Its rearrangements are increasingly recognized as potent oncogenic drivers. In gastric plexiform fibromyxoma, *MALAT1*-derived regulatory elements (e.g., TATA box, ETS1 motifs) act as a strong promoter when fused to *GLI1*, driving expression of a truncated *GLI1* transcript.[13] The resulting protein lacks key regulatory domains, leading

to constitutive Hedgehog pathway activation and increased cell proliferation.[14] Additionally, in *TFEB*-rearranged renal cell carcinoma, translocation places *TFEB* under the control of the *MALAT1* promoter, causing marked *TFEB* overexpression and sustained activation of genes involved in proliferation, metabolism, and tumorigenesis.[15]

We hypothesize that these two genetic events are not isolated but may exert synergistic effects. One plausible model is that the unknown gene activated by the *MALAT1* rearrangement and the downstream signaling pathway activated by the mutant *CSF1R* converge and mutually reinforce each other at a critical nodal point, such as a shared transcriptional regulator or cell-cycle checkpoint. This synergistic interaction could generate potent oncogenic driving forces, ultimately leading to the development of this low-grade mesenchymal tumor with a unique macrophage-like phenotype.

In summary, we present a distinctive tumor characterized by its occurrence in infancy, location in the axillary subcutaneous tissue, histomorphology of a low-grade spindle cell tumor, a unique CD163/CD68-positive macrophage-like immunophenotype, and a co-occurring molecular signature of *CSF1R* mutation and *MALAT1* rearrangement. This tumor cannot be classified into any known existing category. The co-occurring molecular signature of *CSF1R* mutation and *MALAT1* rearrangement has not been reported in the existing literature, which may act synergistically to drive tumorigenesis and progression. Future research aimed at identifying the specific partner gene of the *MALAT1* rearrangement will significantly deepen our understanding of the pathogenesis of this tumor type and lay the groundwork for exploring precision therapies targeting the *CSF1R* pathway.

Acknowledgments

None.

Funding

None.

Conflict of interest

Dr. Anjia Han is an editorial board member of *Journal of Clinical and Translational Pathology*. The authors declare no other conflicts of interest.

Author contributions

Manuscript drafting and image preparation (ML), technical support (YD), study conception and supervision (AH). All authors have approved the final version and publication of the manuscript.

Ethical statement

This study was performed in accordance with the Declaration of Helsinki (as revised in 2024). This case study does not include identifiable patient information. According to institutional policy, this report has been exempted from Institutional Review Board approval and informed consent.

Data sharing statement

All data generated or analyzed during this study are included in this article.

References

[1] Black J, Coffin CM, Dehner LP. Fibrohistiocytic tumors and related neoplasms in children and adolescents. Pediatr Dev Pathol 2012;15(1 Suppl):181–210. doi:10.2350/11-03-1001-PB.1, PMID:22420728.
[2] Knezevich SR, McFadden DE, Tao W, Lim JF, Sorensen PH. A novel ETV6-NTRK3 gene fusion in congenital fibrosarcoma. Nat Genet 1998;18(2):184–187. doi:10.1038/ng0298-184, PMID:9462753.
[3] Griffin CA, Hawkins AL, Dvorak C, Henkle C, Ellingham T, Perlman EJ. Recurrent involvement of 2p23 in inflammatory myofibroblastic tumors. Cancer Res 1999;59(12):2776–2780. PMID:10383129.
[4] Kao EY, Mantilla JG. What's new in soft tissue and bone pathology 2022-updates from the WHO classification 5th edition. J Pathol Transl Med 2022;56(6):385–386. doi:10.4132/jptm.2022.10.18, PMID:36413981.
[5] Dehner CA, Lazar AJ, Chrisinger JSA. Updates on WHO classification for small round cell tumors: Ewing sarcoma vs. everything else. Hum Pathol 2024;147:101–113. doi:10.1016/j.humpath.2024.01.007, PMID:38280658.
[6] WHO Classification of Tumours Editorial Board. Soft tissue and bone tumours. 5th ed. Lyon: International Agency for Research on Cancer; 2020.
[7] Tap WD, Healey JH. Role of colony-stimulating factor 1 in the neoplastic process of tenosynovial giant cell tumor. Tumour Biol 2022;44(1):239–248. doi:10.3233/TUB-220005, PMID:36502356.
[8] Szczepanski J, Westerhoff M, Schechter S. Plexiform Fibromyxoma: A Review and Discussion of the Differential Diagnosis of Gastrointestinal Mesenchymal Tumors. Arch Pathol Lab Med 2025;149(9):e298–e304. doi:10.5858/arpa.2024-0254-RA, PMID:39743931.
[9] Hamilton JA. Colony-stimulating factors in inflammation and autoimmunity. Nat Rev Immunol 2008;8(7):533–544. doi:10.1038/nri2356, PMID:18551128.
[10] Peyraud F, Cousin S, Italiano A. CSF-1R Inhibitor Development: Current Clinical Status. Curr Oncol Rep 2017;19(11):70. doi:10.1007/s11912-017-0634-1, PMID:28875266.
[11] Tap WD, Gelderblom H, Palmerini E, Desai J, Bauer S, Blay JY, *et al*. Pexidartinib versus placebo for advanced tenosynovial giant cell tumour (ENLIVEN): a randomised phase 3 trial. Lancet 2019;394(10197):478–487. doi:10.1016/S0140-6736(19)30764-0, PMID:31229240.
[12] Xu WW, Jin J, Wu XY, Ren QL, Farzaneh M. MALAT1-related signaling pathways in colorectal cancer. Cancer Cell Int 2022;22(1):126. doi:10.1186/s12935-022-02540-y, PMID:35305641.
[13] Hamada T, Higashi M, Yokoyama S, Akahane T, Hisaoka M, Noguchi H, *et al*. MALAT1 functions as a transcriptional promoter of MALAT1::GLI1 fusion for truncated GLI1 protein expression in cancer. BMC Cancer 2023;23(1):424. doi:10.1186/s12885-023-10867-6, PMID:37165307.
[14] Spans L, Fletcher CD, Antonescu CR, Rouquette A, Coindre JM, Sciot R, *et al*. Recurrent MALAT1-GLI1 oncogenic fusion and GLI1 up-regulation define a subset of plexiform fibromyxoma. J Pathol 2016;239(3):335–343. doi:10.1002/path.4730, PMID:27101025.
[15] Argani P, Reuter VE, Zhang L, Sung YS, Ning Y, Epstein JI, *et al*. TFEB-amplified Renal Cell Carcinomas: An Aggressive Molecular Subset Demonstrating Variable Melanocytic Marker Expression and Morphologic Heterogeneity. Am J Surg Pathol 2016;40(11):1484–1495. doi:10.1097/PAS.0000000000000720, PMID:27565001.